PERFORMANCE COMPARISON OF A NOVEL THERMOFLUIDIC ORGANIC-FLUID HEAT CONVERTER AND AN ORGANIC RANKINE CYCLE HEAT ENGINE

Christoph J.W. Kirmse, Aly I. Taleb, Oyeniyi A. Oyewunmi, Andrew J. Haslam, and Christos N. Markides*

Clean Energy Processes (CEP) Laboratory, Department of Chemical Engineering, Imperial College London, London SW7 2AZ, UK
E-mail: c.markides@imperial.ac.uk

* Corresponding Author

ABSTRACT

The Up-THERM engine is a novel two-phase heat engine with a single moving part–a vertical solid piston–that relies on the phase change of a suitable working fluid to produce a reciprocating displacement and sustained thermodynamic oscillations of pressure and flow rate that can be converted to useful work. A model of the Up-THERM engine is developed via lumped dynamic descriptions of the various engine sub-components and electrical analogies founded on previously developed thermoacoustic principles. These are extended here to include a description of phase change and non-linear descriptions of selected processes. The predicted first and second law efficiencies and the power output of a particular Up-THERM engine design aimed for operation in a specified CHP application with heat source and sink temperatures of 360 °C and 10 °C, are compared theoretically to those of equivalent sub-critical, non-regenerative organic Rankine cycle (ORC) engines. Five alkanes (from *n*-pentane to *n*-nonane) are being considered as possible working fluids for the aforementioned Up-THERM application, and these are also used for the accompanying ORC thermodynamic analyses. Owing to its mode of operation, lack of moving parts and dynamic seals, the Up-THERM engine promises a simpler and more cost-effective solution than an ORC engine, although the Up-THERM is expected to be less efficient than its ORC counterpart. These expectations are confirmed in the present work, with the Up-THERM engine showing lower efficiencies and power outputs than equivalent ORC engines, but which actually approach ORC performance at low temperatures. Therefore, it is suggested that the Up-THERM can be a competitive alternative in terms of cost per unit power in low-power/temperature applications, especially in remote, off-grid settings, such as in developing countries where minimising upfront costs is crucial.

1. INTRODUCTION

Primary energy efficiency, leading to a reduced consumption of fossil-fuel reserves and of related emissions to the environment, has been attracting increased attention in recent years. The present paper considers an innovative vapour-phase heat-engine concept termed 'Up-THERM'. The Up-THERM engine was first proposed, designed and tested by company Encontech B.V. (http://www.encontech.nl) and is currently being further developed under the EU FP7 project Up-THERM (http://labor1.wix.com/up-therm) for combined heat and power (CHP) applications. The engine can be said to belong to a class of systems knows as 'thermofluidic oscillators'. Examples of single-phase thermofluidic oscillators include Sondhauss tubes (Sondhauss, 1850), thermoacoustic engines (Ceperley, 1979), Stirling (B. Kongtragool, 2003) and Fluidyne engines (Stammers, 1979). In particular, the Up-THERM engine is a *two-phase* thermofluidic oscillator akin to the 'Non-Inertive-Feedback Thermofluidic Engine' (NIFTE) (Markides and Smith, 2011; Solanki et al., 2012, 2013a,b), but also comprises a single solid piston (Glushenkov et al., 2012; Samoilov et al., 2013) much like gas-phase Stirling engines (rather than the liquid pistons employed in the NIFTE or Fluidyne engines). Similarly to the NIFTE, a constant temperature difference

applied between the hot and cold parts of the Up-THERM device results in the periodic evaporation and condensation of the working fluid in an unsteady thermodynamic cycle. This leads to unsteady oscillations of pressure, temperature, and volume within the engine, and the reciprocating vertical motion of the piston. By transforming the oscillatory movement of the fluid into unidirectional flow through check valves and hydraulic accumulators, power can be extracted by means of a hydraulic motor.

The Up-THERM engine can be thought of as an alternative to the more commercially mature organic Rankine cycle (ORC) engine: by relying on the phase-change of its working fluid, it is suitable for converting low-grade heat to useful mechanical power, and it is an external heat engine that can be used with a variety of heat sources. In particular, it promises *relatively* high efficiencies at low power outputs while being a more affordable solution compared to conventional systems. In this paper, we compare the efficiency and power output of an Up-THERM prime-mover design for a pre-specified CHP application to ORC equivalents, based on operation between the same heat source and sink temperatures, with the same heat input (indicative of scale and cost), and using the same (organic) working fluids.

2. UP-THERM ENGINE CONFIGURATION AND OPERATION

The Up-THERM engine concept is depicted in Figure 1a. The engine consists of a displacer cylinder, a connection tube and a load arrangement. The displacer cylinder comprises the hot and cold heat exchangers, the solid piston, a slide bearing, and a mechanical spring. The piston and cylinder wall together form a 'piston-valve' arrangement. Under operating conditions part of the space above the piston, at the very top of the displacer cylinder, is occupied by the working fluid in the vapour phase, which acts like a gas spring. The load arrangement consists of two check (non-return) valves, two hydraulic accumulators, and a hydraulic motor. The fluid flow directions are illustrated by black arrows.

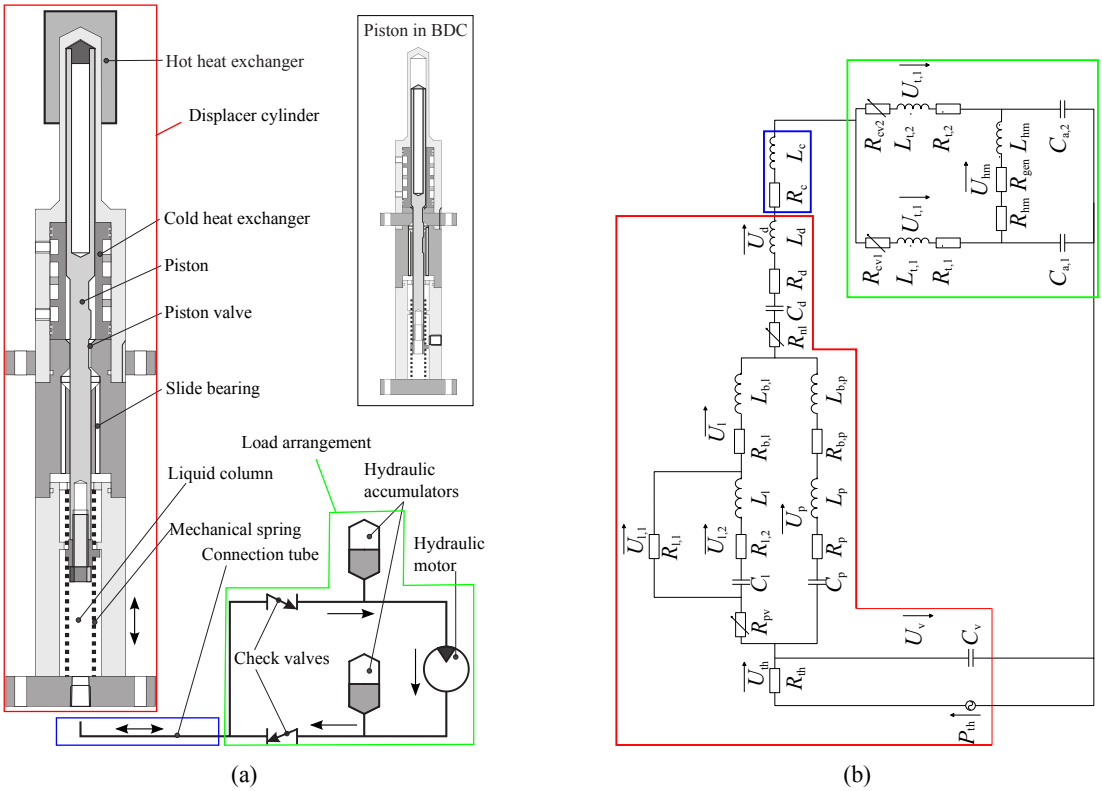

Figure 1: (a) Schematic of the Up-THERM engine with the piston at TDC and BDC (inset). (b) Circuit diagram of the Up-THERM; colours correspond to the engine components in (a).

Consider cyclic operation that starts with the piston at the top dead centre (TDC) position inside the displacer cylinder, as depicted in Figure 1a. The piston valve is open, the mechanical spring fully com-

pressed, and the vapour-liquid (VL) interface is in contact with the surface of the hot heat exchanger (HHX). Liquid working fluid evaporates and thus the pressure in the gas spring increases. This, together with the relaxation of the mechanical spring, leads to a downward movement of the solid piston and of the VL interface. Fluid flows from the compartment above the piston valve into the chamber below it, and into the adjoining connection tube. The piston valve eventually closes preventing continued fluid flow into the lower chamber. The pressure in the upper chamber continues rising, thus generating a pressure difference between both chambers. The pressure difference forces the piston to move downward and the valve re-opens. The pressures above and below the valve are thereby equalized and fluid flows through the valve. Due to the inertia of the piston and fluid, their downward movement continues. They overshoot their equilibrium position halfway between the HHX and cold heat exchanger (CHX).

The vapour, now in contact with the cold CHX surface, begins to condense, while the mechanical spring is compressed. When the piston reaches the bottom dead centre (BDC), the restoring forces of the mechanical spring and decreasing pressure in the gas spring reverse the direction of the piston and VL interface. The piston valve closes again, establishing a similar pressure difference as previously. After re-opening, fluid flows through the valve into the upper chamber while the pressure is equalized. The piston moves further upwards until it reaches the TDC, and the cycle repeats.

During the cycle, liquid oscillates (with zero mean flow) in the connection tube. The oscillating flow is transformed into a unidirectional flow by the two check-valves in the load arrangement, while the hydraulic accumulators act to dampen the amplitude of flow and pressure fluctuations. Thus, a steady unidirectional flow is provided to the hydraulic motor, where work can be extracted from the device.

3. MODEL DEVELOPMENT

3.1 Up-THERM engine

The approach taken for the modelling of the Up-THERM engine concept follows the earlier approaches by Ceperley (1979), Huang and Chuang (1996), and Backhaus and Swift (2000) as applied to thermoacoustic and thermofluidic devices, but also those taken for the modelling of the NIFTE, which is the most closely related device to the Up-THERM since it also exploits a phase-change of the working fluid between hot/cold heat exchangers. Inertial effects were neglected in the original effort of Smith (2004, 2005, 2006), however this early model was later extended to include these effects (Markides and Smith (2011); Solanki et al. (2012)), allowing for more realistic predictions of the operational and performance characteristics of the device. Markides et al. (2013) proceeded to introduce a non-linear temperature profile over the heat exchangers, resulting in further improvements in the predictions of the NIFTE's efficiency. The model was validated against experimental data, showing good agreement with the frequencies and efficiencies reported for an early-stage NIFTE prototype water pump (Solanki et al., 2013b; Markides et al., 2013). This approach (including the non-linear temperature profile) is deemed to be a suitable starting point for the modelling the Up-THERM engine. Full details of the modelling approach employed here for the Up-THERM can thus be found in these references.

Briefly, the engine is divided into sub-components. The dominant thermal or fluid-dynamic process taking place in each of these is modelled using first-order spatially lumped, ordinary differential equations (ODEs). For the following sub-components, we assume small fluctuations around an equilibrium point allowing us to linearize the ODEs: the piston; the slide bearing; the liquid column; the connection tube; the hydraulic accumulators; and the hydraulic motor. Electrical analogies are drawn such that the differential equations governing the dynamic processes are represented by passive electrical components (resistors, inductors, and capacitors). The models of each sub-component are interconnected to form an electrical circuit network that reflects the physical manifestation of the engine; see Figure 1b.

In more detail, force balances on the liquid volume in the connection tube and in the displacer cylinder are employed to derive the electrical analogies for these components. The Reynolds and Wormersley numbers are assumed to be sufficiently low such that quasi-steady, fully developed flow can be assumed. In this case, linearized resistances can be used to represent viscous drag, linearized inductances represent

fluid inertia, and capacitances hydrostatic pressure differences (in the displacer cylinder only):

$$R = \frac{128\mu l_0}{"\pi d^4}; \quad L = \frac{\rho l_0}{A}; \quad C = \frac{A}{\rho g}. \tag{1}$$

A force balance on the piston is combined with the Navier-Stokes equations for the surrounding leakage flow to derive the linearized electrical analogies for these two components. In the slide bearing, the fluid flows through two channels and hence is modelled as a liquid column. The piston slides through a third channel lubricated by a thin working-fluid film and experiences drag. Thus, the electrical components required to model the dynamics of the piston, leakage flow, and slide bearing are:

$$R_{\mathrm{l},1} = \frac{128c_2h_\mathrm{p}\mu}{\pi c_1 c_3}; \quad R_{\mathrm{l},2} = \frac{128c_2h_\mathrm{p}\mu}{\pi c_1\left(c_1 - 2c_2d_\mathrm{p}^2\right)}; \quad C_\mathrm{l} = \frac{\pi^2 c_1\left(c_1 - c_2d_\mathrm{p}^2\right)}{64c_2^2k_\mathrm{ms}}; \quad L_\mathrm{l} = \frac{64c_2^2m_\mathrm{p}}{\pi^2 c_1\left(c_1 - 2c_2d_\mathrm{p}^2\right)};$$

$$R_\mathrm{p} = \frac{64h_\mathrm{p}\mu}{\pi d_\mathrm{p}^2 c_1}; \quad C_\mathrm{p} = \frac{\pi^2 d_\mathrm{p}^2 c_1}{32k_\mathrm{ms}c_2}; \quad L_\mathrm{p} = \frac{32m_\mathrm{p}c_2}{\pi^2 d_\mathrm{p}^2 c_1}; \quad R_{\mathrm{b,p}} = \frac{16\mu h_\mathrm{b}}{\pi^2 d_\mathrm{p}^3\delta}; \quad L_{\mathrm{b,p}} = \frac{4\rho_\mathrm{ss}h_\mathrm{b}}{\pi d_\mathrm{p}^2}; \tag{2}$$

$$L_{\mathrm{b,l}} = \frac{4\rho h_\mathrm{b}}{\pi d_\mathrm{b}^2}; \quad R_{\mathrm{b,l}} = \frac{128\mu h_\mathrm{b}}{\pi d_{\mathrm{b,l}}^4}.$$

In Eq. 2, three geometric constants are used: $c_1 = d_\mathrm{c}^2 - d_\mathrm{p}^2$, $c_2 = \ln\left(d_\mathrm{c}/d_\mathrm{p}\right)$, and $c_3 = c_2\left(d_\mathrm{c}^2 + d_\mathrm{p}^2\right) - c_1$.

The gas springs in the hydraulic accumulators are modelled using the linearized ideal gas law with:

$$C = \frac{V_0}{\gamma P_0}. \tag{3}$$

A torque balance is used to model the losses and inertia in the hydraulic motor. Ohm's law is used to calculate the power $\dot{W}_\mathrm{el}$ that can be extracted from the engine as a function of the flow rate U_hm through the hydraulic motor. The power is dissipated in the resistance R_el which is determined empirically.

$$R_\mathrm{hm} = \frac{16\mu_\mathrm{lub}d_\mathrm{s}^3h_\mathrm{s}}{\pi\varepsilon d^4 d_\mathrm{m}^2}; \quad L_\mathrm{hm} = \frac{8m_\mathrm{m}}{\pi^2 d^4}; \quad \dot{W}_\mathrm{el} = R_\mathrm{gen}U_\mathrm{hm}^2. \tag{4}$$

In addition to the linear descriptions of the aforementioned components, the gas spring above the piston, the piston valve, the two check valves, and the temperature profile over the heat exchangers are modelled non-linearly. The piston valve is described by a non-linear resistance:

$$R_\mathrm{pv} = R_\mathrm{min} + \frac{1}{2}R_\mathrm{max}\left(-\mathrm{H}\left\{P_\mathrm{C,d} - \rho_\mathrm{wfl}gh_\mathrm{pv}\right\} + \mathrm{H}\left\{P_\mathrm{C,d} + \rho_\mathrm{wfl}gh_\mathrm{pv}\right\}\right), \tag{5}$$

using a Heaviside step function $\mathrm{H}\{.\}$, such that the valve opens and closes at the height h_pv.

The check valves and non-linear resistance R_nl in the displacer cylinder are also modelled using Heaviside step functions. The check valves are either open or closed depending on the flow direction U_d:

$$R_\mathrm{cv} = R_{\mathrm{max,cv}}\mathrm{H}\left\{U_\mathrm{d}\right\}, \tag{6}$$

while by introducing the non-linear resistance R_nl it is ensured that the vertical displacement amplitudes of the solid piston and liquid column are not larger than the height of the displacer cylinder itself:

$$R_\mathrm{nl} = R_{\mathrm{max},3}\left(\mathrm{H}\left\{P_\mathrm{C,d} - \rho_\mathrm{wfl}gh_3\right\} + \mathrm{H}\left\{-P_\mathrm{C,d} - \rho_\mathrm{wfl}gh_3\right\}\right). \tag{7}$$

In the above equation h_3 is the maximum height of the liquid column. When reaching this height in the physical engine the piston/liquid column contacts a wall and cannot move further.

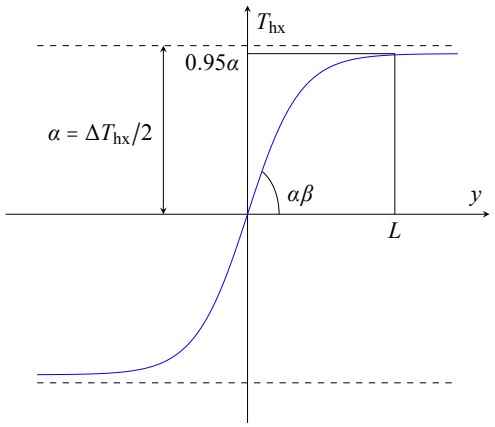

Figure 2: Non-linear temperature profile in the heat exchangers. At length L of the heat exchanger we assume that, by design, the temperature reaches 95% of its saturation value $\alpha = \Delta T_{hx}/2$.

The gas spring above the piston is modelled assuming an isentropic compression and expansion process (PV^{γ} = const.), where γ represents the heat-capacity ratio. Differentiating with respect to time, the temporal variations in the rate of change of pressure $\mathrm{d}P_v/\mathrm{d}t$ of the gas spring can be expressed as:

$$\frac{\mathrm{d}P_v}{\mathrm{d}t} = \frac{\gamma\,(P_0 + P_v)\,U_v}{V_0 + V_v} = \frac{\gamma\,(P_0 + P_v)\left(\frac{P_{th} - P_v}{R_{th}} - U\right)}{V_0 + V_v}\,. \tag{8}$$

The interaction between the fluid at the vapour-liquid interface and the heat exchanger walls is the only nominally active thermal process in the device (corresponding to the thermal domain indicated by the subscript 'th' in Figure 1b), and is explained in more detail in Markides et al. (2013). As the vapour-liquid interface moves far away from (midway between) the equilibrium position between the CHX and HHX, it is assumed that the temperature on the heat exchanger wall T_{hx} is described by a non-linear static relationship that exhibits saturation at long distances from the equilibrium position:

$$T_{hx} = \alpha \tanh(\beta y)\,, \tag{9}$$

where y is the distance of the vapour-liquid interface from the equilibrium position (see Figure 2) and $\alpha\beta$ is the gradient of the profile at equilibrium. Figure 2 illustrates the non-linear temperature profile.

The second law (exergy) efficiency is used here as a performance measure of the Up-THERM engine. It compares the work output of the cycle to the exergy input, and can be calculated from:

$$\eta_{ex} = \frac{\int R_{gen} U_{hm} \mathrm{d}V_{hm}}{\int P_{th} \mathrm{d}V_{th}}\,, \tag{10}$$

where $V_{hm} = \int U_{hm}\mathrm{d}t$ is the volumetric displacement in the hydraulic motor and $V_{th} = \int U_{th}\mathrm{d}t$ the 'equivalent' entropy flow (referred to the fluid domain, hence the volumetric conversion) due to thermal energy transfer to the working fluid over a cycle (Markides and Smith, 2011).

Finally, the first law (thermal) efficiency of the engine is calculated from:

$$\eta_{th} = \eta_C \eta_{ex}\,, \tag{11}$$

where η_C is the Carnot efficiency based on the average (external) heat-source and sink temperatures.

As stated earlier, we consider here the performance of a specific Up-THERM prime-mover design for a defined CHP application with a heat-source inlet temperature of 360 °C and a heat-sink inlet temperature of 10 °C, and with five alternative working fluids (*n*-pentane to *n*-nonane). This engine design and choice working-fluid properties fixes all system parameters, and allows the system of ODEs that describe the device's operation to be solved from which the performance indicators of interest can be evaluated.

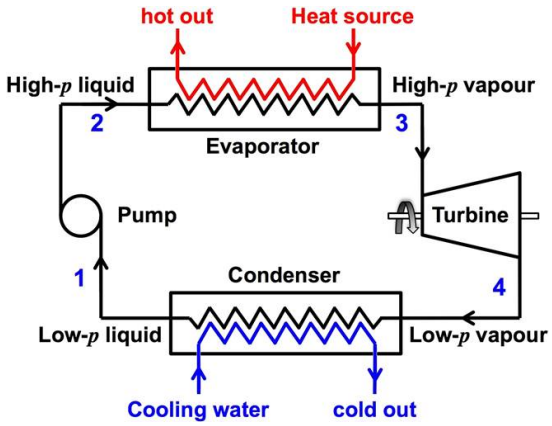

Figure 3: Simple schematic diagram of a non-regenerative ORC engine.

3.2 Organic Rankine cycle engine

A simple schematic of an ORC engine is presented in Figure 3. The working fluid is pumped from a saturated liquid at State 1 to State 2 before being pre-heated and vapourized in the evaporator with thermal energy taken from a hot fluid stream that acts as the heat source. For the purposes of maintaining our comparison, the working fluid remains in the sub-critical region throughout, and exits the evaporator as a saturated liquid; it is not superheated as there is little possibility to superheat in the Up-THERM engine. Moreover, superheating the working fluid during heat addition has been shown to be detrimental to ORC performance in some cases (Chen et al., 2010; Oyewunmi et al., 2014). The high-pressure vapour (State 3) generates power in an expander. The low-pressure vapour is then condensed to State 1, completing the cycle. The key processes of the cycle are described for completeness below.

The power required to pump the working fluid from State 1 to State 2 is:

$$\dot{W}_{\text{pump}} = \dot{m}_{\text{wfl}} \left(h_2 - h_1\right) = \dot{m}_{\text{wfl}} \left(h_{2\text{s}} - h_1\right) / \eta_{\text{is,pump}} \,, \tag{12}$$

with $\eta_{\text{is,pump}}$ being the isentropic efficiency of the pump, which is taken as 75%.

The heat extracted from the heat source is transferred to the working fluid assuming no heat losses and with a minimum pinch temperature difference of 10 °C in the evaporator. The heat addition process is assumed to be isobaric, thus the rate of heat input from the heat source is given by:

$$\dot{Q}_{\text{in}} = \dot{m}_{\text{wf}} \left(h_3 - h_2\right) = \dot{m}_{\text{hs}} \, c_{p,\text{hs}} \left(T_{\text{hs,in}} - T_{\text{hs,out}}\right) . \tag{13}$$

The expander is assumed to have an isentropic efficiency $\eta_{\text{is,exp}}$ of 75%. Hence, the power generated on expanding the working fluid is:

$$\dot{W}_{\text{exp}} = \dot{m}_{\text{wf}} \left(h_3 - h_4\right) = \eta_{\text{is,exp}} \, \dot{m}_{\text{wf}} \left(h_3 - h_{4\text{s}}\right) . \tag{14}$$

Most of the working fluids considered here are ‘dry’ and thus exit the expander in the superheated-vapour state. Therefore, heat is rejected as the working fluid is first de-superheated and then condensed to a saturated liquid isobarically. The rate of heat transferred to a cooling stream is given as:

$$\dot{Q}_{\text{out}} = \dot{m}_{\text{wf}} \left(h_4 - h_1\right) = \dot{m}_{\text{cs}} \, c_{p,\text{cs}} \left(T_{\text{cs,out}} - T_{\text{cs,in}}\right) . \tag{15}$$

Finally, the thermal efficiency of the cycle is calculated from:

$$\eta_{\text{th}} = \frac{\dot{W}_{\text{net}}}{\dot{Q}_{\text{in}}} = \frac{\dot{W}_{\text{exp}} - \dot{W}_{\text{pump}}}{\dot{Q}_{\text{in}}} \,, \tag{16}$$

based on which an exergy efficiency η_{ex} can be determined via η_{C} as before.

The present study considers, from a purely theoretical thermodynamic perspective, the performance of equivalent ORCs to the proposed Up-THERM engines based on operation with the same working fluids, heat source/sink temperatures and heat inputs (indicative of scale/cost).

4. RESULTS AND DISCUSSION

Based on the above models, we proceed now to estimate the expected thermal and exergy efficiencies and power output from the Up-THERM heat engine, and to compare this with equivalent organic Rankine cycle (ORC) engine performance. For this purpose, we consider a heat-source stream inlet temperature of 360 °C and a heat-sink stream inlet temperature of 10 °C. The temperature drop/rise between the inlet and outlet in both heat exchangers is set to 30 °C; again this is done in order to match the external temperatures available to the ORC to those that are known to be available to the Up-THERM cycle. Since the flow rates and temperatures of the heat-source streams are similar in both systems, the heat inputs are therefore also similar, and any difference in power output reflects a different engine efficiency.

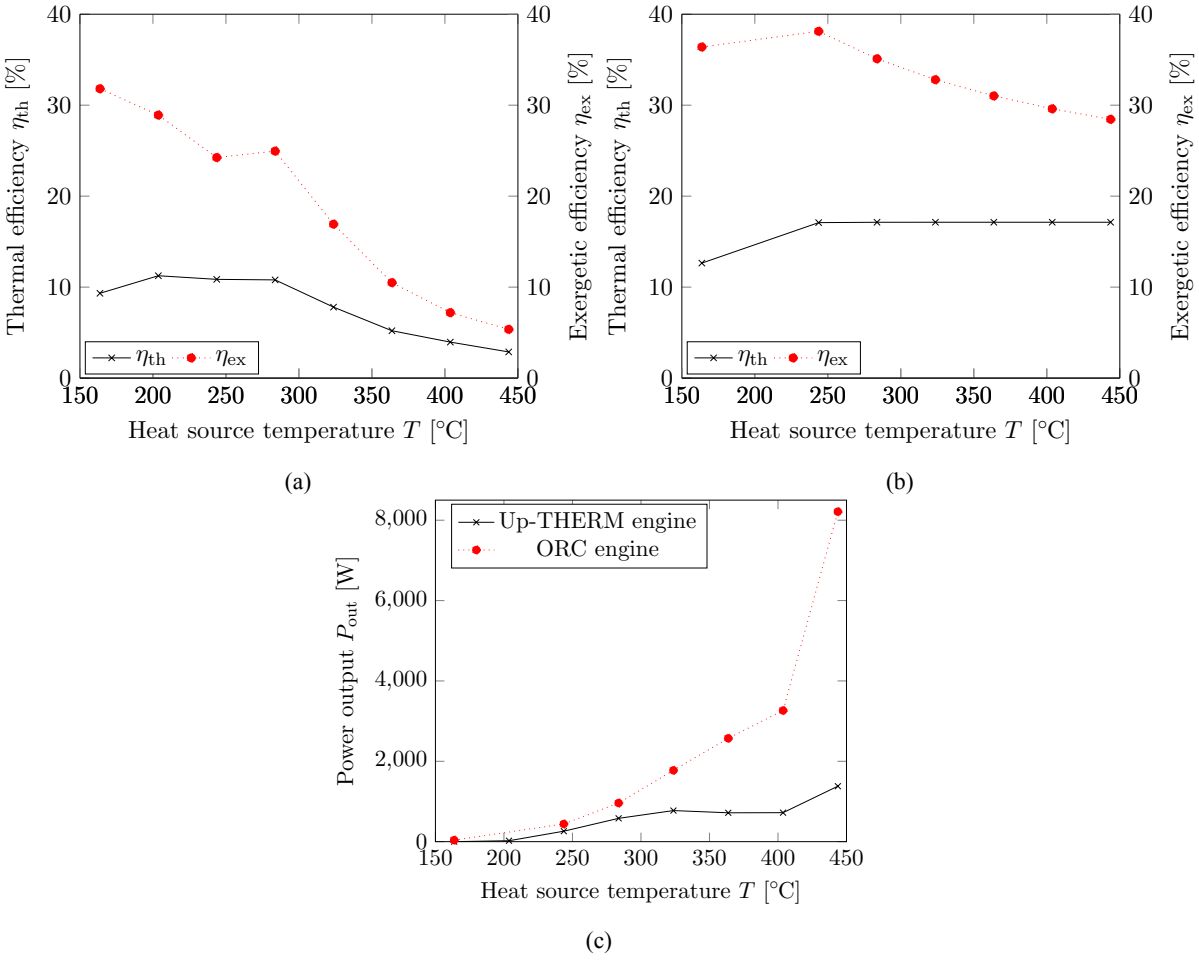

Figure 4: (a) Up-THERM efficiencies for different heat-source temperatures with *n*-hexane; (b) ORC efficiencies corresponding (a); and (c) Up-THERM and ORC net power-outputs.

Firstly we consider the two systems operating with the same working fluid (*n*-hexane) across a range of heat-source temperatures with the same heat sink; all other Up-THERM parameters (except those influenced by the change in equilibrium temperature and pressure) are kept constant. It is important to note from Figure 4(a), that as the heat-source temperature increases the efficiency of the Up-THERM engine first improves (at low temperatures) and then deteriorates again, even though the power output increases monotonically as demonstrated in Figure 4(c). (As the backpressure is increased the amplitudes of the pressure and volume oscillations throughout the system also increase, which leads to an increased flow rate through the hydraulic motor and hence to an increased power output.) At the lowest temperatures the predicted efficiency and power output of the Up-THERM approaches that of the ORC. This suggests that the Up-THERM may offer a competitive proposition when used with low-grade heat sources.

Table 1: Thermal and exergy efficiencies and power output as calculated by the Up-THERM and equivalent ORC engine models for five *n*-alkane working fluids.

	Up-THERM					ORC				
Working Fluid	η_{ex} [%]	η_{th} [%]	$\dot{W}_{net}$ [W]	$\dot{m}_{hs}$ [kg/s]	p_0 [bar]	η_{ex} [%]	η_{th} [%]	$\dot{W}_{net}$ [W]	$\dot{m}_{wf}$ [kg/s]	P_{23} [bar]
Pentane	5.37	2.97	1110	0.55	28.2	28.2	15.2	6090	0.073	30.4
Hexane	11.5	6.37	785	0.018	14.1	31.8	17.1	2250	0.020	27.1
Heptane	21.4	11.9	659	0.081	7.51	33.6	18.1	1080	0.080	24.4
Octane	19.1	10.6	195	0.027	4.13	34.3	18.5	366	0.0024	22.3
Nonane	18.7	10.3	47.2	0.0067	1.02	35.2	19.0	93	0.00055	19.2

Nevertheless, we are interested here in a particular CHP application for the Up-THERM where the heat-source temperature is relatively high (360 °C). Table 1 lists the main performance indicators of interest, namely the thermal and exergy efficiencies and power outputs, predicted by the Up-THERM and equivalent ORC engines models for a selection of working fluids. Additionally, the operating equilibrium/backpressure of the Up-THERM engine for each working fluid, the corresponding evaporation pressure for the ORC engine, and the (common) heat-source fluid-stream flow-rate and working-fluid flow-rate used in the ORC for maximum power are given. When the heavier alkanes are used in the Up-THERM this results generally in a higher efficiency, but a reduced power output due to the lower heat-input from the source. This is due to the lower gain and lower (pressure/flow) oscillation amplitudes that the heavier-hydrocarbon Up-THERM systems experience, given that the external temperature difference across which the device operates is fixed. Pentane is associated with the highest power output, in both the Up-THERM and ORC engines, at least for this application; however, the efficiencies of this working fluid are the lowest. For the Up-THERM, thermal efficiencies of up to 12% and exergy efficiencies of up to 21% (*n*-heptane), and power-outputs of up to 1.1 kW (*n*-pentane) are predicted.

It is clear that the ORC engine outperforms the Up-THERM engine in terms of power output and efficiency for all working fluids, and especially when the lighter hydrocarbons are used. This is a consequence of the relatively high temperature of the heat source in the presently investigated CHP prime-mover application (as identified previously in the discussion relating to Figure 4(c)). Both the power output and efficiencies of the ORC engine are about $2-5$ times higher compared to that of the Up-THERM, depending on the working fluid. Nevertheless, this is a respectable performance from what is a non-optimized Up-THERM design, and also in light of the far lower capital and maintenance costs associated with this technology. Although not on-par in terms of our performance, the Up-THERM appears an interesting technology in terms of performance per unit cost.

5. CONCLUSIONS

In his work, a simple dynamic model of a novel two-phase thermofluidic oscillator featuring a single solid piston termed Up-THERM was developed. The sub-components of the engine are: the displacer cylinder with hot and cold heat exchangers and a solid piston; the connection tube, which links the displacer cylinder with a load arrangement; the load arrangement with hydraulic accumulators, check valves and a hydraulic motor, where power can be extracted from the cycle. The engine was described by a series of first-order spatially lumped ordinary differential equations (ODEs). For some components the ODEs were linearized. Components with a crucial impact on the performance of the engine were described non-linearly. The engine performance was examined with five alkanes as the working fluid. Specifically, the thermal and exergy efficiencies, as well as the power output of a particular Up-THERM engine design aimed for operation as a prime mover in a specified CHP application were evaluated for heat source and sink temperatures of 360 °C and 10 °C. The results were compared theoretically to those of equivalent sub-critical, non-regenerative organic Rankine cycle (ORC) engines. For this Up-THERM engine, thermal efficiencies of up to 12% and exergy efficiencies of up to 21% (*n*-heptane), and power-

outputs of up to 1.1 kW (*n*-pentane) were predicted. The power output and efficiencies of the ORC engine are about 2 − 5 times higher, depending on the working fluid. Thermofluidic oscillators, like the Up-THERM engine, are potentially cheaper to construct than currently available technologies such as ORCs. Since they have less moving parts they also offer the prospect of greater reliability and longevity. We have demonstrated that these advantages can be obtained while maintaining similar performance in terms of efficiency and power output. Accordingly, the Up-THERM engine represents an exciting new technology, particularly in the context of power generation in the developing world.

NOMENCLATURE

C	capacitance	$(\mathrm{m^4s^2/kg})$
d	diameter	(m)
g	gravitational acceleration	$(\mathrm{m/s^2})$
h	height, enthalpy	(m), (J/kg)
$H\{.\}$	Heaviside step function	(-)
k	spring constant	(N/m)
L	inductance	$(\mathrm{kg/m^4})$
P	pressure fluctuations around equilibrium pressure	(Pa)
R	resistance	$(\mathrm{kg/m^4s})$
U	flow rate	$(\mathrm{m^3/s})$
V	volume fluctuations around equilibrium volume	$(\mathrm{m^3})$
$\dot{W}$	power	(W)
α	half the temperature difference between HHX and CHX	(-)
γ	heat capacity ratio	(-)
δ	gap between piston and slide bearing	(m)
ε	gap between shaft and motor	(m)
μ	dynamic viscosity	$(\mathrm{m^2/s})$
ρ	density	$(\mathrm{kg/m^3})$

Subscript

0	equilibrium
a	hydraulic accumulator
b	slide bearing
c	connection tube
cv, pv	check valve, piston valve
d	displacer cylinder
el	electric
ex	exergy
gen	generator
hm	hydraulic motor
hx	heat exchanger
l	leakage flow
lub	lubricant
m	motor
min, max	minimum, maximum value
ms, vs	mechanical spring, vapour spring
nl	non-linear
p	piston
s	shaft
t	tube
th	thermal

wfl liquid working fluid

REFERENCES

B. Kongtragool, S. W. (2003). A review of solar-powered Stirling engines and low temperature differential stirling engines. *Renewable and Sustainable Energy Reviews*, 7(2):131–154.

Backhaus, S. and Swift, G. W. (2000). A thermoacoustic-Stirling heat engine: Detailed study. *Journal of the Acoustical Society of America*, 107(6):3148–3166.

Ceperley, P. H. (1979). A pistonless Stirling engine-The traveling wave heat engine. *Journal of the Acoustical Society of America*, 66(5):1508–1513.

Chen, H., Goswami, D. Y., and Stefanakos, E. K. (2010). A review of thermodynamic cycles and working fluids for the conversion of low-grade heat. *Renewable and Sustainable Energy Reviews*, 14(9):3059–3067.

Glushenkov, M., Sprenkeler, M., Kronberg, A., and Kirillov, V. (2012). Single-piston alternative to Stirling engines. *Applied Energy*, 97(0):743–748.

Huang, B. J. and Chuang, M. D. (1996). System design of orifice pulse-tube refrigerator using linear flow network analysis. *Cryogenics*, 36(11):889–902.

Markides, C. N., Osuolale, A., Solanki, R., and Stan, G.-B. V. (2013). Nonlinear heat transfer processes in a two-phase thermofluidic oscillator. *Applied Energy*, 104(0):958–977.

Markides, C. N. and Smith, T. C. B. (2011). A dynamic model for the efficiency optimization of an oscillatory low grade heat engine. *Energy*, 36(12):6967–6980.

Oyewunmi, O. A., Taleb, A. I., Haslam, A. J., and Markides, C. N. (2014). An assessment of working-fluid mixtures using SAFT-VR mie for use in organic Rankine cycle systems for waste-heat recovery. *Computational Thermal Sciences*, 6(4):301–316. ID: 50af28c84073a421.

Samoilov, A., Kirillov, V., Kuzin, N., Kronberg, A., Glushenkov, M., Taleb, A. I., and Markides, C. N. (2013). An external combustion heat engine with phase-change working fluid. In *Proceedings of the 13th UK Heat Transfer Conference, UKHTC2013*.

Smith, T. C. (2004). Power dense thermofluidic oscillators for high load applications. In *Proceedings of the 2nd International Energy Conversion Engineering Conference, Providence (RI)*, pages 1–15.

Smith, T. C. (2005). Asymmetric heat transfer in vapour cycle liquid-piston engines. In *Proceedings of the 12th International Stirling Engine Conference and Technology Exhibition*, pages 302–314.

Smith, T. C. (2006). Thermally driven oscillations in dynamic applications. *PhD thesis, University of Cambridge, Cambridge, UK*.

Solanki, R., Galindo, A., and Markides, C. N. (2012). Dynamic modelling of a two-phase thermofluidic oscillator for efficient low grade heat utilization: Effect of fluid inertia. *Applied Energy*, 89(1):156–163.

Solanki, R., Galindo, A., and Markides, C. N. (2013a). The role of heat exchange on the behaviour of an oscillatory two-phase low-grade heat engine. *Applied Thermal Engineering*, 53(2):177–187.

Solanki, R., Mathie, R., Galindo, A., and Markides, C. N. (2013b). Modelling of a two-phase thermofluidic oscillator for low-grade heat utilisation: Accounting for irreversible thermal losses. *Applied Energy*, 106(0):337–354.

Sondhauss, C. (1850). Ueber die schallschwingungen der luft in erhitzten glasröhren und in gedeckten pfeifen von ungleicher weite. *Annalen der Physik*, 155(1):1–34.

Stammers, C. W. (1979). The operation of the Fluidyne heat engine at low differential temperatures. *Journal of Sound and Vibration*, 63(4):507–516.

ACKNOWLEDGEMENT

The research leading to these results has received funding from the 7th Framework Programme of the European Commission, grant agreement number 605826.